3-D Finite Element Modeling of Brain Edema: Initial Studies on Intracranial Pressure Using Comsol Multiphysics

X.G.Li[1], H.von Holst[1,2], J.Ho[1] and S.Kleiven[1]
[1]KTH - Royal Institute of Technology, Division of Neorunic Engeering
[2]Karolinska Institute, Department of Clinical Neuroscience
*Corresponding author: Alfred Nobels Allé 10 141 52 Huddinge, Sweden , xiaogai.li@sth.kth.se

Abstract: Brain edema is one of the most common consequences of serious traumatic brain injuries which is usually accompanied with increased intracranial pressure (ICP) due to water content increment. A three-dimensional finite element model of brain edema is used to study intracranial pressure in this paper. Three different boundary conditions at the end of cerebral spinal fluid (CSF) were used to investigate the boundary condition effects on the volume-pressure curve based on the current model. Compared with the infusion experiments, results from the simulations show that exponential pressure boundary condition model corresponds well with the experiments.

Keywords: Brain edema, Intracranial pressure(ICP), Consolidation theory, Finite element model.

1 Introduction

Brain edema is one of the most common consequences of serious traumatic brain injuries because of the enhancement of water content and thus the increased brain volume. Brain compensation mechanisms, such as increased CSF absorption, compression of the venous thin-walled vessels, and excessive displacement of CSF downwards to the spinal canal exist when ICP is increasing [10]. However, once the brain compensation mechanisms have been exhausted, intracranial pressure will increase exponentially with the intracranial volume. Previous research shows that the consolidation theory provides a solution for studying the fluid flow in the brain and has been widely used in hydrocephalus and brain edema studies in early researches [16, 17, 18, 19, 21]. More recent studies on hydrocephalus using simple geometries for analytical solution in order to understand the mechanism lies behind [11, 12], 2D slices [3, 15] and 3D finite element (FE) brain models have been developed [5]. At present, no 3D finite element model exists for brain edema simulation. Two different kinds of brain edema coexist after brain injury, "cytotoxic edema" and "vasogenic edema", however, different types dominate during different time after trauma. The mechanism of "vasogenic edema" is relatively well understood due to breakdown of BBB (Blood-Brain-Barrier) and this results in water accumulation at the neurosis place [4, 20]. In this paper, a three-dimensional finite element model of brain edema is used to study ICP using Comsol Multiphysics [1]. ICP is usually mentioned as the pressure in the ventricle clinically, thus pore pressure at ventricle in the model is taken as ICP. Three different boundary conditions at the end surface of the CSF were used to investigate the boundary condition effects on the volume-pressure curve based on the current model. Due to the similarity between the water accumulation at edema place and the infusion of fluid into the intracranial space in the infusion experiments [6], we used the volume pressure curve in the experiments to evaluate the model. However, infusion rate was scaled down in order to simulate the much slower process of water accumulation in edema. CSF is modeled as a poroelastic material, but it's unclear about the permeability, thus a parametric study has been performed using the constant pressure boundary condition model for both infusion rate and permeability of CSF.

2 Poroelastic modeling in Comsol Multiphysics

Poroelastic governing equations for fully saturated pore fluid flow are based on force equilibrium equations and conservation of fluid mass applied to Darcy's law. This can be

implemented in Comsol Multiphysics using the predefined poroelaticity application mode which combines Solid mechanics module with Darcy's law module. It's a fully bidirectional coupling in which the mechanical equilibrium equations and fluid continuity equation should be satisfied simultaneously. In this quasi-static simulation, static mechanical equilibrium equation for solid phase should be satisfied at each time step, and transient analysis was used for fluid phase to account for the delaying effects of finite permeability and storage response [2, 7].

Specifically about the equations implemented in Comsol Multiphysics [1], solid phase governing equation:

$$-G\nabla^2 u_i - \frac{G}{(1-2\nu)}\frac{\partial u_k}{\partial x_i x_k} = -\alpha\frac{\partial(\rho_f g z)}{\partial x_i} \quad (1)$$

Where z is the elevation potential, since we didn't take hydrostatic pressure into consideration, which will result $z = 0$ and total pressure should be equal to excess pressure. $G = E/2(1+\nu)$ is the shear modulus with E as the Young's modulus and ν as Poisson's ratio which are all drained value. In Solid mechanics module, pore pressure effects were taken into consideration by including initial pressure as following:

$$\sigma_{ij} = \sigma'_{ij} - \alpha p \delta_{ij} \quad (2)$$

σ_{ij} is the total stress. σ'_{ij} is the effective stress. Under this condition, in the GUI of Solid mechanics module, boundary loading of stress actually is the total stress instead of effective stress and one need to be cautious when adding pressure boundary condition. The governing equation in Darcy's law application mode is a pure pressure formulation:

$$S_\varepsilon \frac{\partial p}{\partial t} + \vec{\nabla}\cdot(-\frac{\kappa}{\mu}\vec{\nabla}(p+\rho_f g z)) = -\alpha\frac{\partial}{\partial t}\epsilon_{kk} + Qs \quad (3)$$

An additional loss term containing time rate change in strain $-\alpha\frac{\partial}{\partial t}\epsilon_{kk}$was added to liquid source function $Q_s$which represent the solid phase effect on the fluid phase. $S_\varepsilon$is the constrained specific storage coefficient, which is related to the bulk modulus of the fluid K_f , solid grain K_s and void ratio n:

$$\frac{1}{M} = \frac{\alpha - n}{K_s} + \frac{n}{K_f} \quad (4)$$

3 Model

3.1 Geometry and Mesh

The mesh of the model is a simplified version modified from the mesh in paper [14] as shown in figure 1 which includes the gray matter, white matter, corpus callosum, brain stem, ventricles, cerebrospinal fluid (CSF) et al. We need to mention that ventricles and aqueduct are also filled with CSF and the CSF component we named here represents only the component that covers the outer surface of the whole brain. CSF in the ventricles and the outer component CSF are connected by the newly created aqueduct. Two elements originally from the white matter with volume of $7.29 \times 10^{-7} m^3$ were moved to a new part and defined as edema where fluid accumulates. A simplified neck was created, together with spinal cord servers as a reservoir and represents the lower part of the CSF circulation system. Due to the limitation in importing the mesh into Comsol multiphysics, original hexahedral elements were splitted into tetrahedral elements.

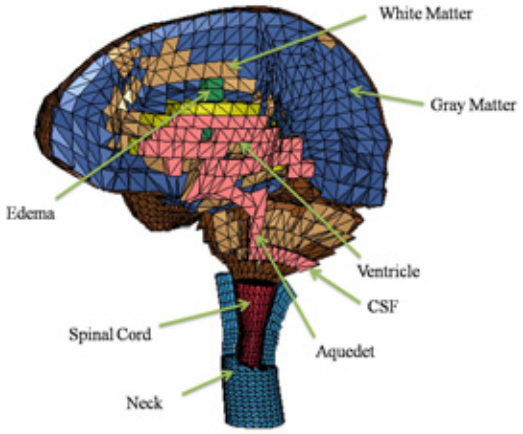

Figure 1: Finite element model of brain.

3.2 Parameter evaluation

Brain tissue including CSF are modeled as poroelastic material, while the neck is taken as linear elastic material. Parameter values used in the model was discussed in the previous paper [8] as listed in the Appendix. Brain tissue contains about 78% of water and is usually taken as incompressible for both fluid and brain solid grain. However, although the

brain itself is nearly incompressible, vasculature or capillary in the brain is about 5% [13], when ICP increases, blood will be expelled from intracranial space, which may make it reasonable to treat the brain cell as slightly compressible to compensate for this. In the model, we used a compressibility of $1/K_s = 1.09 \times 10^7\, 1/Pa$ for solid grain, which is 50 times more compressible than water.

3.3 Loading and boundary conditions

Evidence suggests that a large amount of edema fluid is accumulated in the necrotic brain tissue within the central area of the contusion and this contributes to the early massive edema with progressive elevation of the ICP. Thus a water source term Qs was added in the edema elements with a constant rate of $80.57cc/min$ modified proportionally from the rate in the experiment of $3.87cc/min$ according to a human brain volume of $V_{brain} = 1.499 \times 10^{-3}m^3$ in the model from the estimated volume of the dog brain $V_{dogbrain} = 7.2 \times 10^{-5}m^3$. The infusion in the experiment was relatively fast compared with water accumulation in edema which usually takes days [21]. In the model, the water accumulation rate in edema necrosis was scaled down according to the experimental infusion within 30 s, while in the simulation 3000 s, with a lower infusion rate was used resulting in the same amount of relative water volume change. Source term Qs added in edema part in equation (3) represents the water volume accumulation in the edema place per unit time per unit edema volume. Although in the animal experiment the water was pumping into the subarachnoid space, while in the model water was added in the necrotic brain tissue, similar volume pressure curve should be expected.

Boundary conditions in the fluid phase in the models are zero flux and pressure boundary condition. Zero flux BC gives:$\nabla p = 0$ and no fluid is allowed to flow out through the boundary. Pressure BC gives: $p = p_0$, p_0 can be a constant value or a function. Under pressure boundary condition, the pressure is added in the fluid phase in the model, as discussed in Section 2, the corresponding boundary loading at Solid mechanics module GUI should be total stress according to equation (2) gives $\sigma_{ij} = -\alpha p \delta_{ij}$ if the effective stress is equal to zero, which means that all the pressure loading is added on the fluid phase at the end surface of CSF. Initial conditions for fluid phase is set to $1066\, Pa$ which is the same as the base pressure as in the infusion experiments.

3.4 Boundary condition effect studies

For solid phase, same boundary condition is used for all three models. The outer surface of the CSF was defined as the skull and fixed, while the outer surface of the neck was set free. Figure 2 shows the end surface of the CSF where three different boundary conditions for fluid phase were tested: zero flux, constant pressure $1066\, Pa$ and an exponentially increasing pressure.Pictures in Appendix show the pressure distribution of ICP in three different BC models.

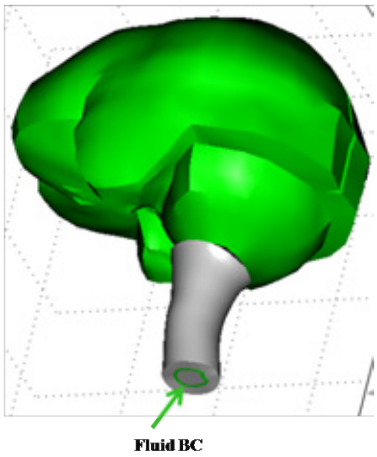

Figure 2: Different BCs at the end surface of CSF.

Results from the simulation indicate that the pressure is almost homogeneously distributed in the brain except at place around edema. The curve clearly shows the much different pressure distribution depending on three different boundary conditions. The original curve in paper [6] was redrawn to relate the infusion volume per unit brain volume to be comparable with the results from the simulations.

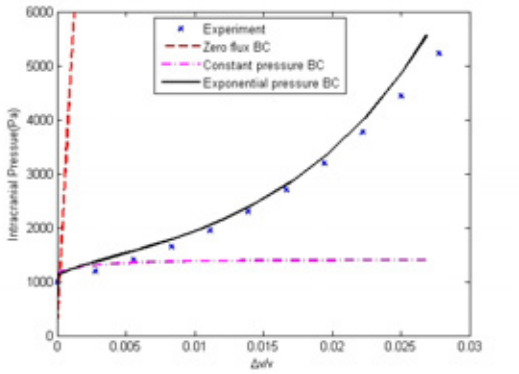

Figure 3: The influence of different boundary conditions on ICP.

From figure 3, with zero flux BC, ICP is linearly increasing with the infusion volume and is much higher than in the experiment. For constant pressure BC, ICP increases slowly at the early stage of infusion and reaches to an almost constant level after some time, since most of the the infused water flows out via the CSF end surface. When an exponential pressure was added, ICP increases exponentially and corresponds well with the experiment.

3.5 Parametric studies on CSF permeability using constant pressure BC model

CSF actually behaves as fluid, however, in this paper, it's also treated as poroelastic material but a higher void ratio $n = 0.9$ was used in order to represent that most of the poroelastic CSF is filled with water. CSF permeability in the model is taken as $1.426 \times 10^{-10} m^2$ and aqueduct is one order lower in order to compensate the much wider aqueduct in the model than in reality. However, it's unclear about the value of permeability should be used. Thus a parametric study using different order of permeability was studied using values from $1.426 \times 10^{-9} m^2$ to $1.426 \times 10^{-13} m^2$ for the constant pressure BC model.

Figure 4 shows the results of the ICP at t = 3000 s with different CSF permeability values which shows that shows that the higher permeability results in lower ICP. However, when permeability is higher than the order of -10, it doesn't affect much. Also, if much higher permeability is used, because of the much difference between the permeability of other tissues such as gray matter in the order of -16 which may cause numerical problems in the model, thus we assume that the value of CSF permeability used in the model is reasonable and reflect fluid property of CSF using poroelastic material.

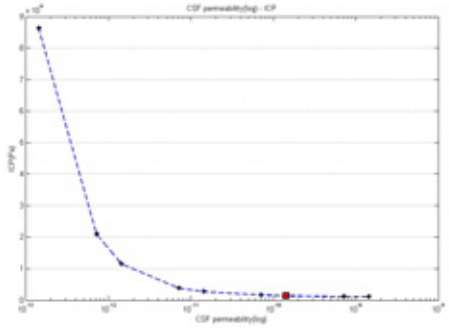

Figure 4: ICP at t = 3000 s with different CSF permeability(log).

3.6 Infusion rate effect studies

In this model, infusion rate was scaled down and used a simulation time of 3000 seconds instead of 30 seconds in order to simulate slower process in edema. This value is also unclear, thus different infusion rate was used in the constant pressure BC model in order to investigate the effect.

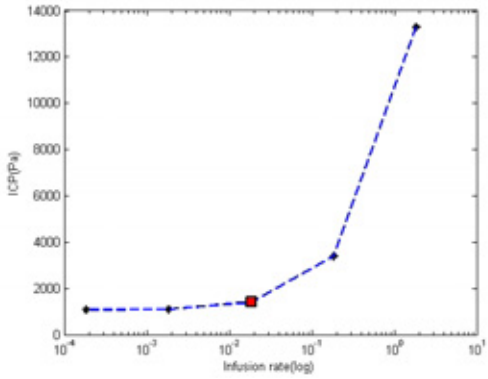

Figure 5: ICP at t = 3000 s with different CSF permeability(log).

Figure 5 shows ICP at end of infusion with different infusion rate, higher infusion rate will results much higher pressure. This is because under high infusion rate, water accumulates at edema place doesn't have time to dissipate. Especially at edema place, the deformation is

unrealistically large due to water trapped at edema place. However, if scaled down to lower than 3000 seconds, infusion rate will not affect much on the volume-pressure curve. Thus we assume the infusion rate in the model is reasonable.

4 Discussions

Poroelastic theory was used to study the intracranial pressure distribution due to brain edema. In all three boundary conditions, the pressure is homogeneously distributed in the whole brain except at the place round edema, which may be due to the nearly incompressibility for both the brain and the CSF while the aqueduct helps connecting the CSF and ventricles to simulate the CSF circulation. However, the pressure at the ventricle differs significantly using these three different boundary conditions of the end surface of the CSF based on the current model. ICP is increasing linearly with the volume increased to a very high value, even the simplified neck is free to expand, seems this doesn't compensate enough. For constant pressure boundary condition, ICP is increasing at the early stage of infusion and come to a steady state after sometime since most of the fluid flows out of the system and constant pressure BC doesn't provide enough resistance to the system. A exponentially increasing pressure BC is added and results corresponds well with the experiments which may due to increasing higher pressure BC provides larger resistance to the system, less fluid flow out and also because of the much high permeability of the boundary pressure can be transmitted to the ventricle in a quite short time. Due to the time scaling between the experiments and simulation, parametric studies were performed on CSF permeability and infusion rate, results show that the CSF permeability and infusion rate used in the models are reasonable. In this paper, only boundary conditions were studied. However, the brain compensation system is much more complex. More factors needed to be taken into consideration, such as CSF generation and absorption, and especially absorption is usually found to be pressure depended [9]. In the current model, zero flux boundary condition model shows a clear linear relationship between the infusion volume and pressure. However, when brain is under compression, blood can be expelled from the vessels, and this reflects in the mathematical model can be related to the non constant storage term S_ε. Also, during edema, water accumulation mechanisms are much more complex than the constant infusion. There are also many limitations in the model. All the simulation shows a linear relationship between the infusion volume and pressure. Research show that the permeability is deformation dependent [11]. However, in the model, a constant value was used and large deformations were not considered. Whether it's reasonable to use a poroelastic material for the CSF can also be questioned, although set to higher porosity and permeability. However, poroelastic theory shows a great potential in studying pressure distribution due to edema in the brain.

References

[1] Comsol AB, *Comsol multiphysics (2008) comsol 3.5a.*

[2] M A.Biot, *General theory of three-dimensional consolidation*, Journal of Applied Physics **12** (1941), 155–164.

[3] A.Pena, M.Bolton, and H.Whitehouse, *Effects of brain ventricular shape on periventricular biomechanics: a finite element analysis*, Neurosurgery **45** (1999), 107–118.

[4] A.Unterberg, J.Stover, and B.Kress, *Edema and brain trauma*, Neuroscience **129** (2004), 1021–1029.

[5] T D.Roy, A.Wittek, and K.Miller, *Biomechanical modelling of normal pressure hydrocephalus*, J Biomech **41** (2004), 2263–2271.

[6] F.Sklar and I.Elashvili, *The pressure-volume function of brain elasticity*, J Neurosurg **47** (1977), 670–679.

[7] Herbert F.Wang, *Theory of linear poroelasticity with applications to geomechenics and hydrogeology*, Princeton University Press.

[8] X G.Li, H von.Holst, J.Ho, and S.Kleiven, *Three dimensional poroelastic simulation of brain edema: Initial studies on intracranial pressure.*

[9] Michael J.Albeck, Svend E.Borgesen, and Flemming.Gjerris et al., *Intracranial pressure and cerebrospinal fluid outflow conductance in healthy subjects*, J Neurosurg **74** (1991), 597–600.

[10] J.Goffin, *Brain oedema and intracranial pressure*, IUTAM Proceedings on Impact Biomechanics: From Fundamental Insights into Applications **124** (2005), 379–382.

[11] M.Kaczmarek, R P.Subramaniam, and S R.Neff, *The hydromechanics of hydrocephalus: steady state solutions for cylindrical geometry*, Bull Math Biol **59** (1997), 295–323.

[12] D N.Levine, *The pathogenesis of normal pressure hydrocephalus: A theoretical analysis*, Bull Math Biol **61** (1999), 875–916.

[13] P.Basser, *Interstitial pressure, volume and flow during infusion into brain tissue*, Microvasc Res **44** (1992), 143–165.

[14] S.Kleiven, *Predictors for traumatic brain injuries evaluated through accident reconstructions*, Stapp Car Crash J **51** (2007), 1–35.

[15] S.Momjian and D.Bichsel, *Nonlinear poroplastic model of ventricular dilation in hydrocephalus*, J Neurosurg **109** (2008), 100–107.

[16] T.Nagashima, B.Horwitz, and S I.Rapoport, *A mathematical model for vasogenic brain edema*, Adv Neurol **50** (1990), 317–326.

[17] T.Nagashima, N.Tamaki, and S.Matsumoto, *Biomechanics of hydrocephalus: a new theoretical model*, Neurosurgery **21** (1987), 898–904.

[18] T.Nagashima, T.Shirakuni, and S I .Rapoport, *A two-dimensional, finite element analysis of vasogenic brain edema*, Neurol Med Chir **30** (1990), 1–9.

[19] T.Nagashima, Y.Tada, and S.Hamano, *The finite element analysis of brain oedema associated with intracrnial meningiomas*, Acta Neurochirurgica Suppl **51** (1990), 155–57.

[20] Y.Katayama and T.Kawamata, *Edema fluid accumulation within necrotic brain tissue as a cause of the mass effect of cerebral contusion in head trauma patients*, Acta Neurochir Suppl **86** (2003), 323–327.

[21] Y.Tada and T.Nagashima, *Modeling and simulation of brain lesions by the finite-element method*, IEEE Eng.Med.Biol **13** (1990), 497–503.

Acknowledgements

This study was supported by School of Technology and Health, KTH – Royal Institute of Technology and we would like to acknowledge support provided by Chinese Council Scholarship (CSC) for the first author. We also want to acknowledge COMSOL support group for the technical support .

Appendix

Pressure distribution under different boundary conditions

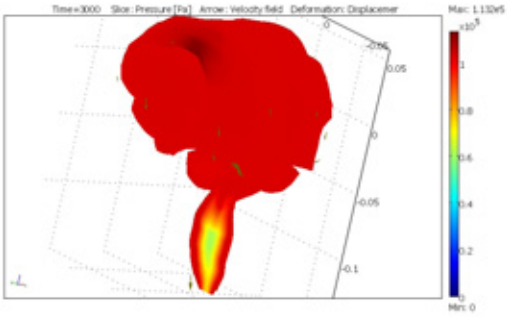

Figure 6: Zero flux BC pressure distribution at t = 3000 s.

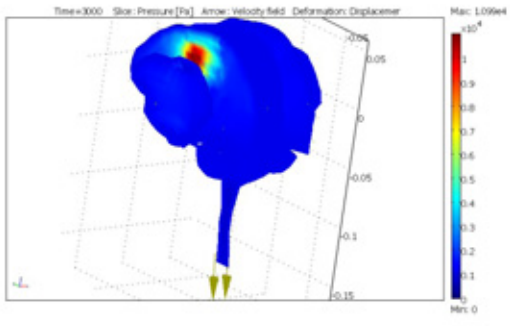

Figure 7: Constant pressure BC pressure distribution at t = 3000 s.

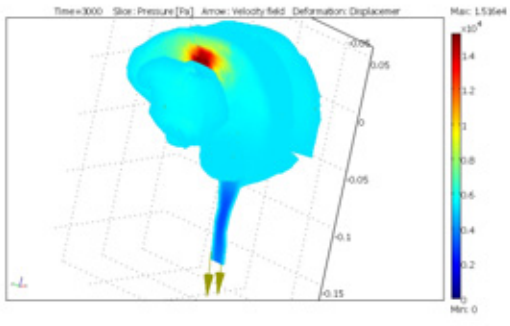

Figure 8: Constant pressure BC pressure distribution at t = 3000 s.

Items	$\kappa(m^2)$	$S_\varepsilon(1/Pa)$	$E(Pa)$	ν
WM	1.426×10^{-14}	1.8356×10^{-8}	9.010×10^3	0.35
GM & Other tissue	1.426×10^{-16}	1.8356×10^{-8}	9.010×10^3	0.35
Aqueduct	1.426×10^{-11}	2.6941×10^{-9}	9.010×10^3	0.35
CSF	1.426×10^{-10}	2.6941×10^{-9}	9.010×10^3	0.35
Ventricle	1.426×10^{-10}	2.6941×10^{-9}	9.010×10^3	0.35
Neck	–	–	4.2×10^5	0.42

Table 1: Parameter values used in the model.